Regular Article

ANALYTICAL AND BIOANALYTICAL CHEMISTRY RESEARCH

Published by the Iranian Chemical Society

Anal. Bioanal. Chem. Res., Vol. 9, No. 1, 59-71, January 2022.

Voltammetric Determination of Famotidine Using a Bilayer of Electrodeposited Gold Nanodendrites and Mercapto-propanioc Acid

Haneie Salehniya, Mandana Amiri* and Khadijeh Nekoueian

Department of Chemistry, University of Mohaghegh Ardabili, Ardabil, Iran

(Received 4 January 2021 Accepted 29 July 2021)

Due to vital essence of medicine dosage monitoring within therapeutic range, a simple, rapid, high performance, sensitive and environmentally friendly electrochemical sensor was designed and used to diagnose low concentrations of famotidine, a histamine-2 blocker, at pharmaceutical products and biological fluids. In this work, a simple, fast response and efficient voltammetic sensor was designed using the functionalized dendrite-like gold nanostructures with 3-mercapto-propanioc acid (3-MPA/Au-DNSs). Electrochemical studies confirmed well the efficiency of the surface modified glassy carbon electrode (GCE) with 3-MPA/Au-DNSs on amplification of response signal in the presence of famotidine in an applicable linear concentration range of 3.0×10^{-7}-1.0×10^{-5} M. The limit of detection was evaluated to be 3.33×10^{-8} M (for S/N = 3) under the optimum conditions. The modified GCE with 3-MPA/Au-DNSs was successfully applied in determination of famotidine in real samples such as human serum and pharmaceuticals with recoveries of 104.8% and 100.90%, respectively.

Keywords: Famotidine, Dendrite-like gold nanostructures, Electrochemical sensor, Serum sample

INTRODUCTION

Famotidine acts as a histamine-2 blocker by reducing the gastric acid secretion from the Parietal cells. Famotidine is prescribed in treatment of Zollinger-Ellison syndrome and gastro esophageal reflux disease [1]. Monitoring the levels of pharmaceutical compounds in biological fluids is considered as an essential and vital need to keep medicine dosage within therapeutic range (safe and effective dosage) [2] that drives scientists to investigate and develop various analytical techniques such as high performance liquid chromatography [3,4], gas chromatography [5], capillary zone electrophoresis [6], spectrophotometry [7-10], spectrofluorimetry [11], liquid chromatography/tandem mass spectrometry [12] and electrochemical and optical (bio)sensors [1,2,13-15]. Among various analytical methods, electrochemical sensing techniques have gained high popularity due to their interesting advantages such as simplicity, portability, low cost, fast response, environmentally friendly procedure, high sensitivity and selectivity [16]. The electrochemical sensors, which were used in analysis of famotidine, are mostly based on using unmodified electrode materials including pyrolytic carbon film [17], pencil graphite electrode [15], graphite electrode [18], and dropping mercury electrode [19].

There are few reports about using modified electrodes for detection of famotidine in literature such as modified carbon paste electrode with flower-like nickel hydroxide nanosheets, dated back to 2020 [13]. Regarding development of mercury-free electrochemical detection methods of famotidine as a reliable alternative for conventional analysis methods such as chromatography and spectroscopy, in present research work for the first time, GCE surface was modified with functionalized dendrite-like gold nanostructures with 3-mercapto-propanioc acid bilayer to determine low concentration of famotidine with high sensitivity.

Electrode material modification is considered as a

*Corresponding author. E-mail: mandanaamiri@uma.ac.ir

promising method to enhance sensitivity and selectivity of the electrochemical (bio)sensors. In recent decade, a wide range of nanomaterials such as carbon nanomaterials [20-22], nanocomposites [23,24], nanoporous materials [25,26] and especially metal nanostructures [27,28] have been used in design and fabrication of novel and high performance electrochemical sensors [29].

Among various electrode materials, gold nanostructures with a good biocompatibility demonstrate high potential to catalysis charge transport mechanisms and determine a target analyte due to their fascinating optical, electrical and conductivity characteristics [30].

The electrocatalytic performance of gold nanostructures is strongly related to their structures and morphologies [31-33]. Among various forms of gold nanostructures, such as gold nanoparticles, nanorods and nanoplates, gold dendritic nanostructures (Au-DNSs) have demonstrated better electrocatalytic activity and higher adsorption-active sites regarding their superior active surface area and higher porosity structure [34,35]. Electrochemical deposition method has been known as an efficient, simple, fast and environmentally friendly synthesizing method, adjusting the properties of gold nanostructures by controlling morphology [34,36]. Interesting properties of Au-DNSs have made them a highly qualified candidate for fabricating (bio)sensors. Rafatmah *et al*. synthesized and electrodeposited Au-DNSs on the surface of glassy carbon electrode in one step simply, fast and without using any chemical reductant. The rate of charge transport was significantly boosted at modified electrodes with Au-DNSs that resulted in higher sensitivity and selectivity [37].

According to the literature, functionalization of gold nanostructures with thiol compounds is as an effective method to amplify electrocatalytic activity of gold nanostructures. High affinity of gold nanostructures for forming covalent bonds to sulphur (S) atoms has made gold nanostructures as reliable substrates for deposition of thiol compounds *via* Au-S interaction. Thiol functionalization of gold nanostructures at electrode surface boosted the effective surface area, facilitated the charge transport and developed sensing application [38-40].

Here, the surface of GCE was easily modified with Au-DNSs by using an electrochemical deposition method. Then, the electrodeposited Au-DNSs were functionalized with 3-mercapto-propanioc acid (3-MPA) by soaking the modified GCE with Au-DNSs (Au-DNSs/GCE) in 3-MPA solution through Au-S bonds. The fabricated modified electrode (3-MPA/Au-DNSs/GCE) was characterized and studied using scanning electron microscopy, diffuse reflectance spectroscopy, electrochemical impedance spectroscopy and cyclic voltammetry methods. Then, 3-MPA/Au-DNSs/GCE was used to determine trace values of famotidine. The 3-MPA/Au-DNSs on the GCE demonstrated high electrocatalytic activity toward electro-oxidation of famotidine rooting in Au-DNSs with superior surface area and electroconductivity. In this detection method, the amine groups of famotidine can be conjugated with the carboxylic terminated groups of 3-MPA at 3-MPA/Au-DNSs/GCE. The signal response at 3-MPA/Au-DNSs/GCE was clearly higher than that of the bare GCE. The effect of various experimental parameters such as pH of voltammetric solution, scan rate, the concentration of 3-MPA and adsorption time were studied and optimized. Finally, 3-MPA/Au-DNSs/GCE was used in determination of famotidine in pharmaceutical and clinical samples, successfully.

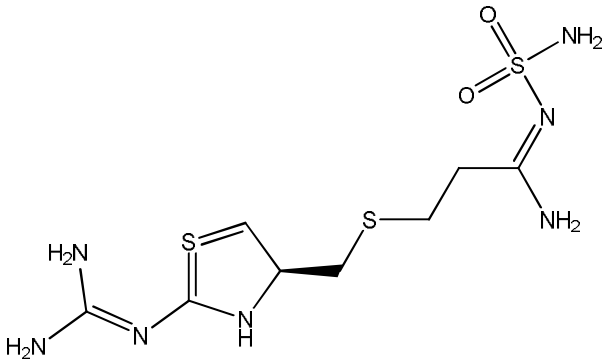

Scheme 1.The chemical structure of famotidine

EXPERIMENTAL

Materials

$HAuCl_4 \cdot 3H_2O$ was purchased from Sigma-Aldrich, USA, NaOH (99%), NaH_2PO_4 (99.99%), K_2HPO_4 (99.99%) and 3-mercaptopropionic acid ($C_3H_6O_2S$) (3-MPA) (≥ 98%) were obtained from Merck, Germany. Doubly distilled deionized water was used for preparing all aqueous

solutions. Famotidine was obtained from Tehrandaro company, Iran (> 99%).

Instruments

Electrochemical experiments were conducted by using a μ-autolabIII potentiostat/galvanostat, Metrohm, Switzerland. In a three-electrode setup, GCE (3.0 mm diameter) as working electrode, a KCl-saturated calomel reference electrode (SCE), and a Pt wire as the counter electrode were employed. The pH of buffer solutions (supporting electrolyte in voltammetric experiments) was measured using a digital pH/mV/Ion meter (Metrohm, Switzerland). The scanning electron microscopy (SEM) was conducted using a ZEISS LEO-1430 VP (Carl Zeiss AG, Jena, Germany). Diffuse reflectance spectra were recorded by using a Scinco S4100 (S. Korea).

Modified Electrode Preparation

Initially, the surface of GCE was polished with alumina powder (smaller than 0.03 μm), rinsed with deionized water. The Au-DNSs were electrodeposited at the surface of GCE in constant anodic potential of -0.4 V for 400 s in a KNO_3 (0.1 M, from Sigma-Aldrich, as a supporting electrolyte) and $HAuCl_4 \cdot 3H_2O$ (6.0 mM, from Aldrich) solution. After that, the modified GCE surface was rinsed with deionized water. Electrodeposition time and applied potential were optimized for better performance of the working electrode.

3-MPA was attached to Au-DNSs by soaking Au-DNSs/GCE into 3-MPA solution (0.2 M) for 5 min immersion time. The immersion time was optimized. The 3-MPA/Au-DNSs/GCE was rinsed with deionized water to omit the unabsorbed 3-MPA. In every experiment, the electrode surface was prepared freshly by casting of 3-MPA at the surface of Au-DNSs/GCE. Cyclic voltammetry technique (CV) and electrochemical impedance spectroscopy (EIS) were applied for electrochemical characterization of 3-MPA/Au-DNSs/GCE.

Preparation of Real Samples (Serum Sample and Pharmaceutical Tablet)

Human serum samples were prepared from healthy individuals and kept frozen until assay. In this procedure, 5 ml of serum was treated with 5 ml of methanol as serum-protein-precipitating agent and was vortexed for 10 min. After that, it was centrifuged. The supernatant liquor was transferred to 25 ml volumetric flask carefully and was diluted with the buffer solution of pH 2.0. To obtain recovery, the standard addition method was used by spiking famotidine to human serum [41].

For preparing pharmaceutical samples, 3 tablets of famotidine (40 mg famotidine per a tablet) weighed and powdered accurately. The powder was transferred into flask and filled to volume with 0.1 M phosphate buffer solution with pH 2.0. After sonication in room temperature, the solutions were filtered and diluted to get final concentration. To calculate the recovery, the standard addition method was applied for determination of famotidine in pharmaceutical tablet.

RESULTS AND DISCUSSION

Characterization of 3-MPA/Au-DNSs/GCE

The SEM technique was used to study the morphology and structure of the electrodeposited Au-DNSs on the surface of GCE. The SEM images of Au-DNSs on surface of GCE were displayed in various deposition time in Fig. 1. The Au-NSs distributed well at GCE surface and demonstrated dendrite-like structures in deposition time 400 s (Fig. 1A). Each Au-DNS, with 1 μm size, was composed of a trunk and several branches. The dendrite-like structure of AuNSs increased the effective surface area on the surface of modified electrode, resulting in higher electrocatalytic activity and higher active binding sites for reacting with suitable functional groups [36]. As can be seen, various deposition times 50 and 200 s led to different morphologies. According to [37] A, B and C, with increasing time, more amounts of gold were deposited on the surface of glassy carbon electrode.

Diffuse reflectance spectroscopy (DRS) is an efficient spectroscopic technique to study the amount of reflected light from solid sample surface. Here, DRS technique was used to study the effect of GCE surface modification with Au-DNSs and 3-MPA/Au-DNSs.

As can be seen in Fig. 2A, similar spectral shapes were recorded for bare GCE, modified GCE with Au-DNSs and

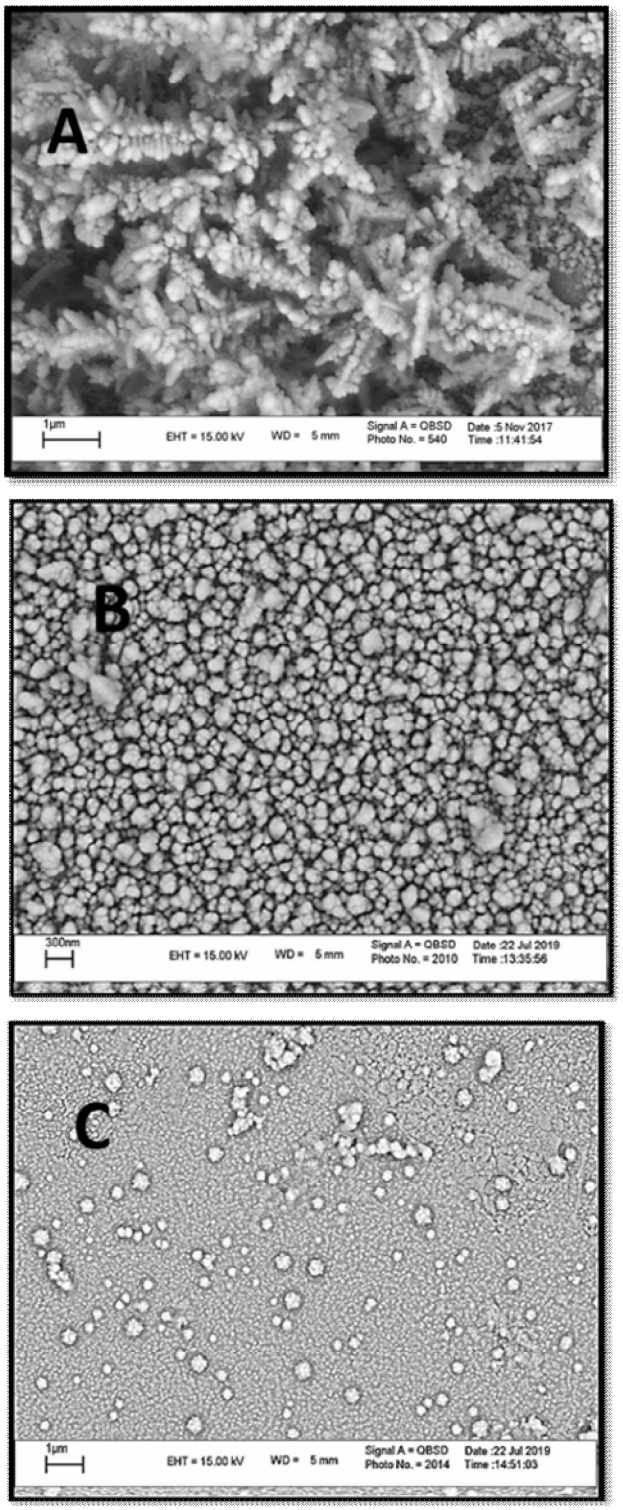

Fig. 1. SEM images of Au-DNSs/GCE in various deposition times: (A) 400, (B) 200, and (C) 50 s.

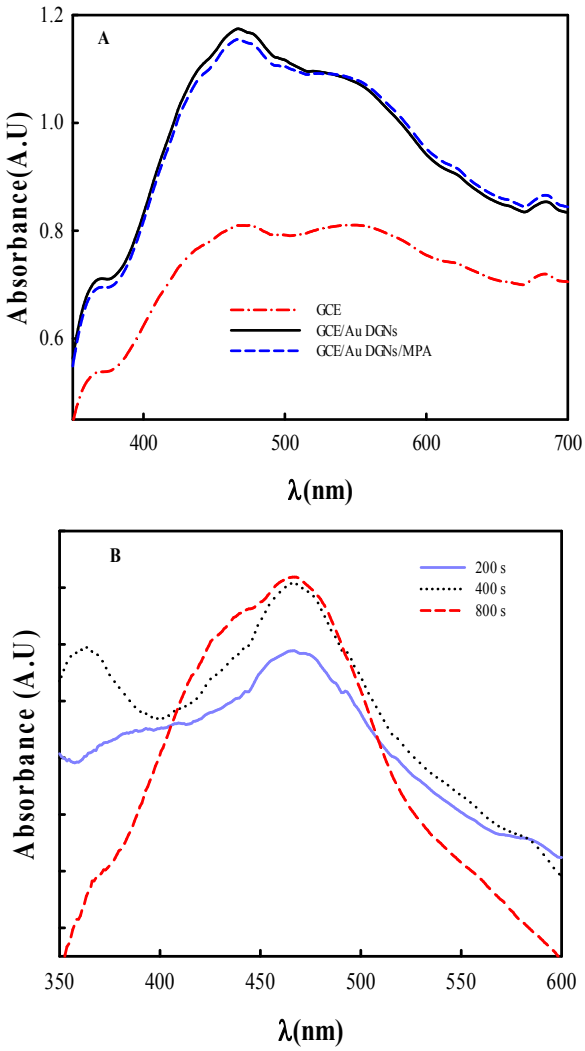

Fig. 2. (A) DRS of bare GCE (dashed-dotted line), Au-DNSs/GCE (solid line), and 3-MPA/Au-DNSs/GCE (dashed line). (B) Effect of different deposition times on the SPR peak of Au-DNSs at Au-DNSs/GCE: 200 s (dashed-dotted line), 400 s (solid line) and 800 s (dashed line).

modified GCE with 3-MPA/Au-DNSs, because of use of same substrate composition with similar chemistry nature, thickness and size through of DRS studies on bare GCE and modified electrodes. There is no significant signal for bare GCE and the obtained surface plasmon resonance (SPR) peaks for both modified GCEs (Au-DNSs and 3-MPA/Au-DNSs) were at the same position 475 nm, which is

attributed to the presence of Au-DNSs [42,43]. It can be suggested that the size and structure of Au-DNSs, deposited and formed at Au-DNSs/GCE and 3-MPA/Au-DNSs/GCE, were similar. The interaction of Au-DNSs with 3-MPA decreased the intensity of SPR peak at 3-MPA/Au-DNSs/GCE.

The effect of electrodeposition time on the SPR peak of Au-DNSs was studied in Fig. 2B. The intensity of absorption peak improved and became readable with increasing deposition time from 200 s to 400 s and then the broadening of SPR peak happened with increasing deposition time from 400 s to 800 s .The broadening of SPR peak can be attributed to the overlap of the transverse and longitudinal SPR bands of the electrodeposited Au-DNSs [43].

Electrochemical Studies

The microscopic area and surface characteristics of GCE and Au-DNSs/GCE were calculated by comparison of the CV responses in 0.1 M phosphate buffer pH 2.0. Capacitance values were obtained 9.25 µF, 28.7 µF for a GCE and Au-DNSs/GCE, respectively. Capacitive current increased significantly, indicated higher active electrode surface area in modified electrode.

The microscopic areas of the modified and the unmodified were obtained by CV using $K_4Fe(CN)_6$ as a probe at different potential scan rates. For a reversible process, the following Randles-Sevcik formula is applied [40]:

$$i_{p,a} = 2.69 \times 10^5 n^{\frac{3}{2}} A C_0 \nu^{\frac{1}{2}} D_0^{\frac{1}{2}} \quad (1)$$

where $i_{p,a}$ shows the anodic peak current, n is the electron transfer number, A is the microscopic surface area of the electrode (cm^2), D_o is the diffusion coefficient ($cm^2\ s^{-1}$), C_o is the bulk concentration of $K_4Fe(CN)_6$ (mol cm^{-3}) and ν is the scan rate (V s^{-1}). The microscopic area was estimated from the slope of the plot of $i_{p,a}$ *vs.* $\nu^{1/2}$. For 5 mM $K_4Fe(CN)_6$ in 0.1 M KCl electrolyte (n = 1 and $D_o = 6.7 \times 10^{-6}$ $cm^2\ s^{-1}$), the electrode surface area of the modified electrode was 0.224 cm^2, and for the unmodified electrode it

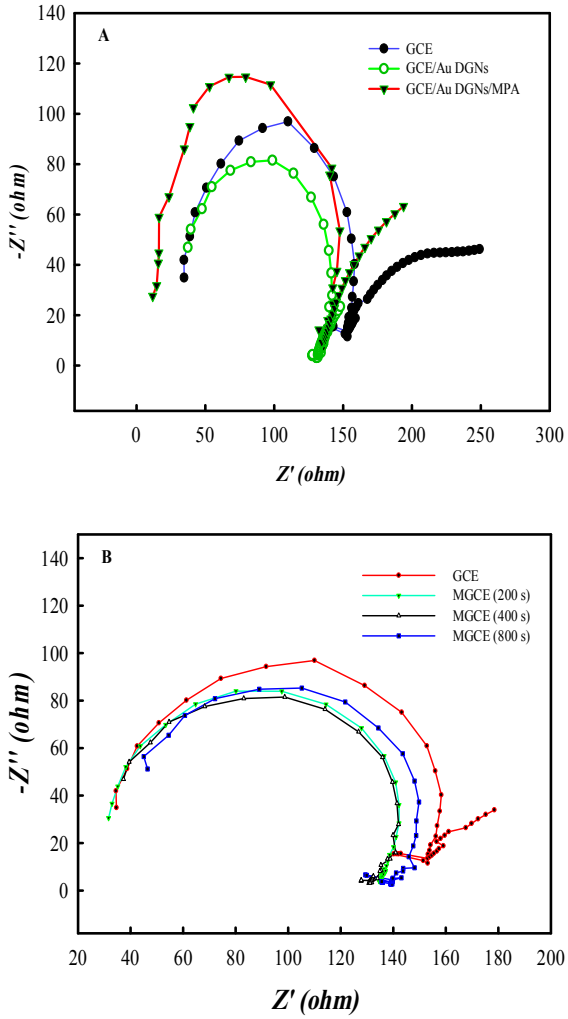

Fig. 3. Nyquist plot for (A) bare GCE (black line), Au-DNSs/GCE (red line), and 3-MPA/Au-DNSs/GCE (green line). (B) Bare GCE (red line) and Au-DNSs/GCE at different deposition times, 200 s (green line), 400 s (black line) and 800 s (blue line), in KCl 0.1 M containing 5 mM [$K_3Fe(CN)_6$/$K_4Fe(CN)_6$] at the formal potential: 0.2 V, frequency range: 1-1000000 Hz.

was 0.064 cm^2. This shows that the microscopic area of the modified electrode increased significantly.

EIS was used to study the effect of modification on the rate of charge transport at electrode surface. Fig. 3A and 3B display the Nyquist plots of $K_3Fe(CN)_6$/$K_4Fe(CN)_6$ at

Table 1. EIS Results for the Bare GCE, Au-DNSs/GCE (at Different Deposition Times 200 s, 400 s and 800 s) and 3-MPA/Au-DNSs/GCE

Electrode	R_{ct} (Ω)	Error	C_{dl} (μF)	Error
Bare GCE	105.7	1.048	1.327	0.0085
Au-DNSs/GCE (200 s)	92.18	0.7454	0.333	0.0068
Au-DNSs/GCE (400 s)	91.60	0.9587	1.329	0.0081
Au-DNSs/GCE (800 s)	95.06	1.048	1.337	0.0085
3-MPA/Au-DNSs/GCE	124.8	3.180	1.235	0.0231

bare GCE (black line), Au-DNSs/GCE (red line), and 3-MPA/Au-DNSs/GCE (green line). The obtained Nyquist plots consisted of two zones: a semicircle plot in high frequency zone related to the kinetic limitations, and a linear plot in a low frequency zone attributed to a diffusion-controlled electrode process. Fig. 3A shows modification of GCE with Au-DNSs decreased the amount of charge transfer resistance (R_{ct}) and boosted the rate of charge transport and conductivity significantly. In Fig. 3B, the effect of electrodeposition time on R_{ct} at Au-DNSs/GCE was compared with bare GCE. The amount of R_{ct} was reduced at Au-DNSs/GCE clearly due to efficiency of Au-DNSs in enhancement of charge transfer rate. The EIS results for Au-DNSs/GCE in different deposition times (200 s, 400 s and 800 s) were compared with bare GCE and 3-MPA/Au-DNSs/GCE at Table 1. The amount of R_{ct} was decreased with increasing deposition time from 200 s to 400 s and then the amount of R_{ct} was increased by increasing deposition time from 400 s to 800 s. Reduction of electron transfer rate can be attributed to the aggregation of Au-DNSs on GCE surface, which can act as a barrier in charge transport mechanism. Also, the amount of R_{ct} increased at 3-MPA/Au-DNSs/GCE, indicated the interaction and attachment of 3-MPA with Au-DNSs.

Cyclic Voltammetric Study of Famotidine at 3-MPA/Au-DNSs/GCE

The efficiency of 3-MPA/Au-DNSs/GCE toward detection of famotidine was evaluated by using CV. The

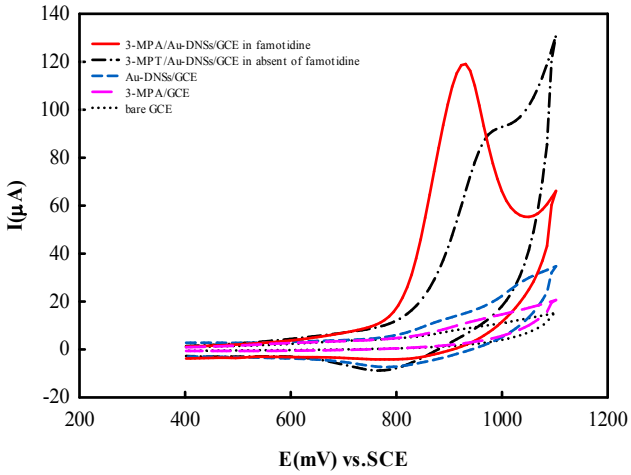

Fig. 4. CVs of bare GCE, 3-MPA/GCE, Au-DNSs/GCE, and 3-MPA/Au-DNSs/GCE in the presence of 0.01 mM famotidine in 0.1 M phosphate buffer solution at pH 2.0, and 3-MPA/Au-DNSs/GCE in 0.1 M phosphate buffer solution at pH 2.0 in the absence of famotidine. The scan rate was 100 mV s^{-1}.

cyclic voltammograms of 0.01 mM famotidine in buffer solution at pH 2.0 (0.1 M phosphate) at the surface of bare GCE, Au-DNSs/GCE, 3-MPA/Au-DNSs/GCE and 3-MPA/GCE were investigated (See Fig. 4). An oxidation peak was recorded for famotidine at the potential of 923 mV with peak current of 0.20 μA at bare GCE. The amount of oxidation peak current was significantly amplified on the

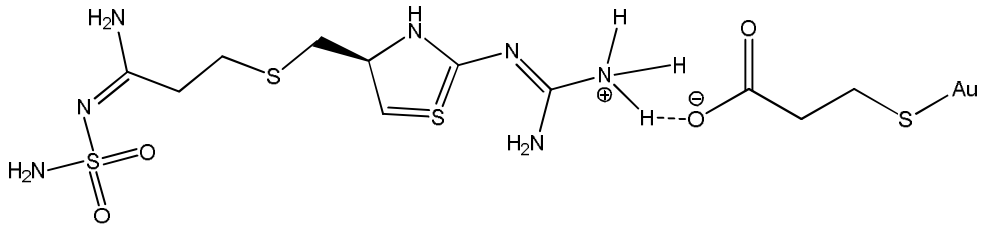

Scheme. 2. The suggested interaction mechanism between 3-MPA and Au-DNSs/GCE and the amine group of famotidine with the carboxylic terminated groups of 3-MPA at 3-MPA/Au-DNSs/GCE surface

surface of 3-MPA/Au-DNSs/GCE and an oxidation peak current of 84.1 μA at potential of 923 mV was appeared. The electrochemical performance of 3-MPA/Au-DNSs/GCE in buffer solution at pH 2.0 (0.1 M phosphate) in the absence of famotidine was studied. An oxidation peak (dashed-dotted line) at potential of 966 mv with a peak current of 19.6 μA was observed, which was different from famotidine oxidation peak clearly.

The anodic peak current of famotidine was raised at the surface of 3-MPA/Au-DNSs/GCE due to Au-DNSs. The advantages of Au-DNSs such as developed specific surface area, amplified charge transfer rate and high affinity to link to S, made Au-DNSs an ideal support for 3-MPA and sensing of famotidine *via* a conjugation between the carboxylic terminated groups of 3-MPA and the amine group of famotidine (Scheme 2). In addition, according to the literature, 3-MPA can amplify the electrocatalytic activity of Au-DNSs [38,39].

Effect of pH on the Electrochemical Response of Famotidine at 3-MPA/Au-DNSs/GCE

The influence of pH on the cyclic voltammograms of 0.01 mM famotidine was studied in buffer solutions with different pHs (2, 3, 6, 7 and 8 with 0.1 M phosphate) and buffer solutions with pHs 4 and 5 (0.1 M acetate) (Fig. 5A). The highest signal was observed in pH 2.0. No oxidation peak current was observed after pH 7.0 (See Fig. 5B). So, further voltammetric studies were conducted at pH 2.0. Regarding Fig. 5C, the oxidation peak potential (E_p) shifted negatively by enhancing pH of the buffer solution. The pH dependency of E_p suggested proton (H^+) participation in electron transfer process. According to the obtained slope: -40.5 mV per pH (Eq. (1)), the equal number of protons and electrons were participating in the famotidine oxidation mechanism.

$$E_p(mV) = -40.5pH + 1.0 \qquad (R^2 = 0.999) \qquad (1)$$

The number of protons (x) and the number of electrons (n) participated in electrooxidation of famotidine can be calculated according to the obtained slope of the $E_p = f(pH)$ dependence, m = -40.5 mV/pH (Eq. (1)), and comparing with the theoretical Nernstian slope (-59x/n mV/pH at 25º C), suggesting that two protons and three electrons (x = 2 and n = 3) participated in the electrooxidation of famotidine.

Effect of 3-MPA Concentration

The effect of 3-MPA concentration on the oxidation peak current of famotidine was studied by voltammetric method (Fig. 6A). In this study, Au-DNSs/GCE was immersed in different 3-MPA concentration levels (0.05 M, 0.1 M, 0.2 M and 0.3 M) for 5 min. Then, the prepared 3-MPA/Au-DNSs/GCE was rinsed and used in voltammetric measurement of 0.01 mM famotidine solution (the scan rate was 100 mV s^{-1}, pH 2.0). The best oxidation peak current was recorded in 2.0 M 3-MPA that was used for further measurements. The response signal was decreased in higher 3-MPA concentration levels, respecting Fig. 6B. This signal reduction can be attributed to the aggregation of 3-MPA on Au-DNSs/GCE surface, which reduced the conductivity and the rate of charge transport at Au-DNSs/GCE surface.

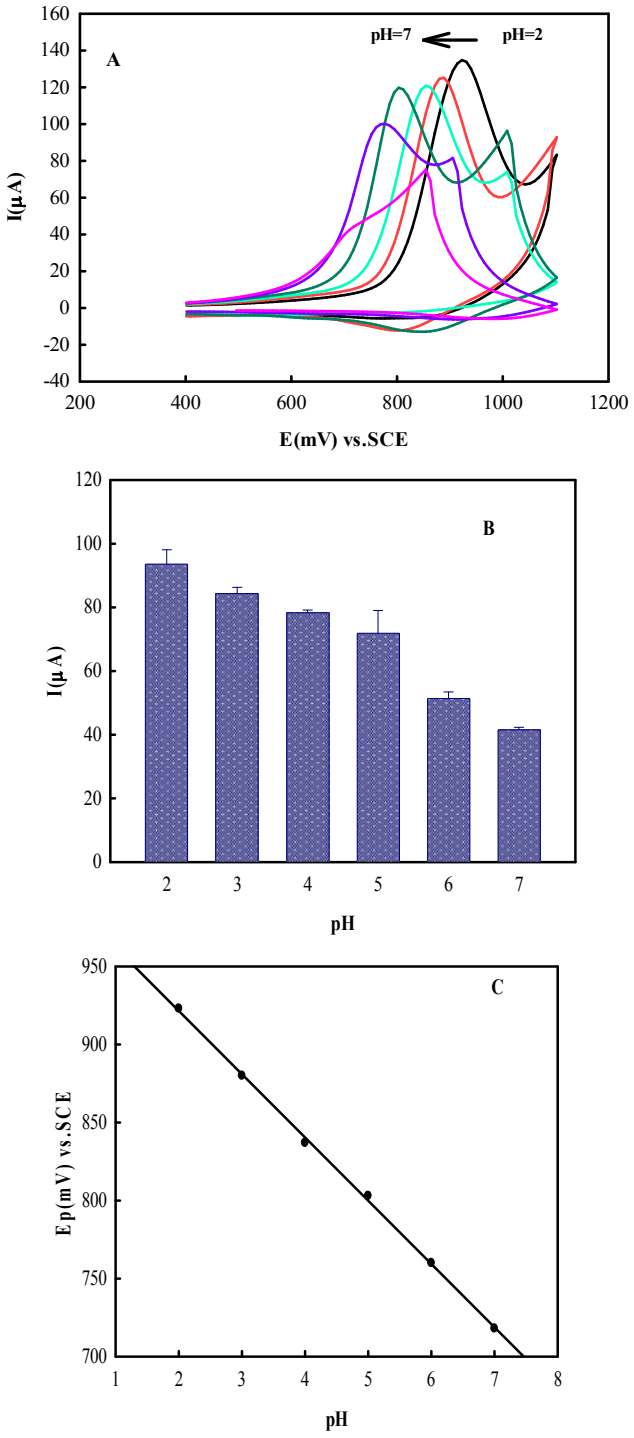

Fig. 5. (A) CVs of 0.01 mM famotidine at 3-MPA/Au-DNSs/GCE in various pHs (2, 3, 4, 5, 6 and 7). (B) Variation of anodic peak potential and (C) anodic peak current *vs*. pH. The scan rate was 100 mV s^{-1}.

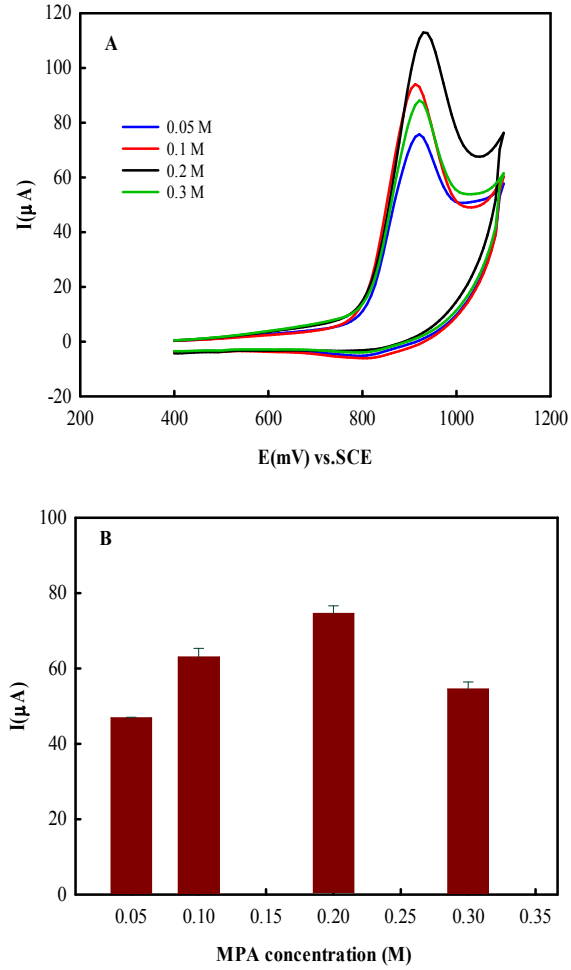

Fig. 6. (A) CVs of famotidine (0.01 mM, in pH 2) at 3-MPA/Au-DNSs/GCE in different 3-MPA concentration levels (0.05 M, 0.1 M, 0.2 M and 0.3 M). (B) Variation of anodic peak current *vs*. different 3-MPA concentration levels (0.05 M, 0.1 M, 0.2 M and 0.3 M). The adsorption time was 5 min and the scan rate was 100 mV s^{-1}.

Effect of Different Aadsorption Times

Effect of different adsorption times of 3-MPA at Au-DNSs/GCE on oxidation peak current of famotidine (0.01 mM, pH 2.0) was investigated by CV (Fig. 7A). In this study, Au-DNSs/GCE was soaked in 0.2 M 3-MPA solution for different adsorption times (2, 5, 15, 30, 60 min). The maximum peak current was recorded at

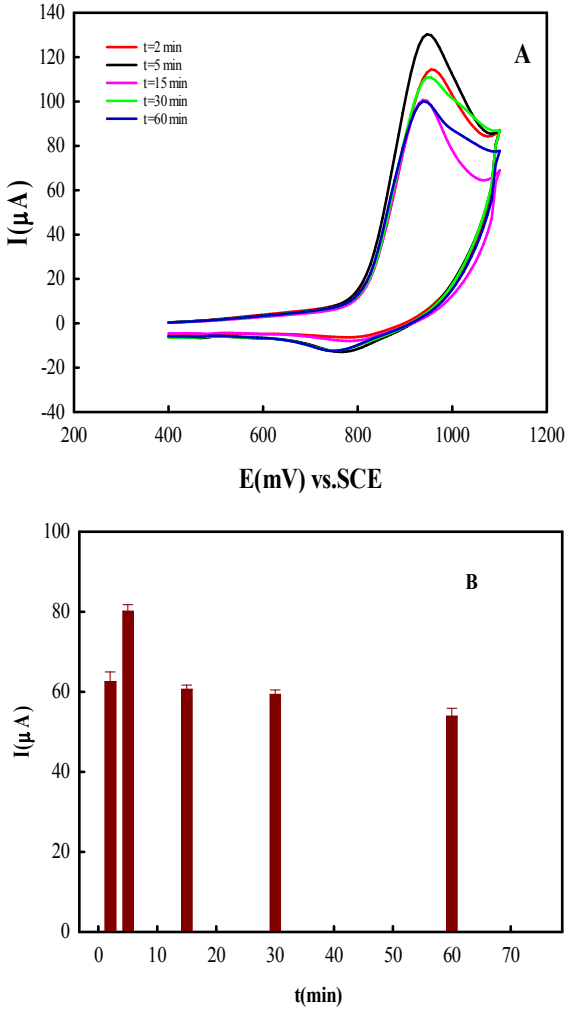

Fig. 7. (A) CVs of 0.01 mM famotidine at 3-MPA/Au-DNSs/GCE (in pH 2 and at different adsorption times 2, 5, 15, 30, 60 min). The scan rate was 100 mV s^{-1}. (B) Variation of anodic peak current *vs.* different adsorption times 2, 5, 15, 30, 60 min)

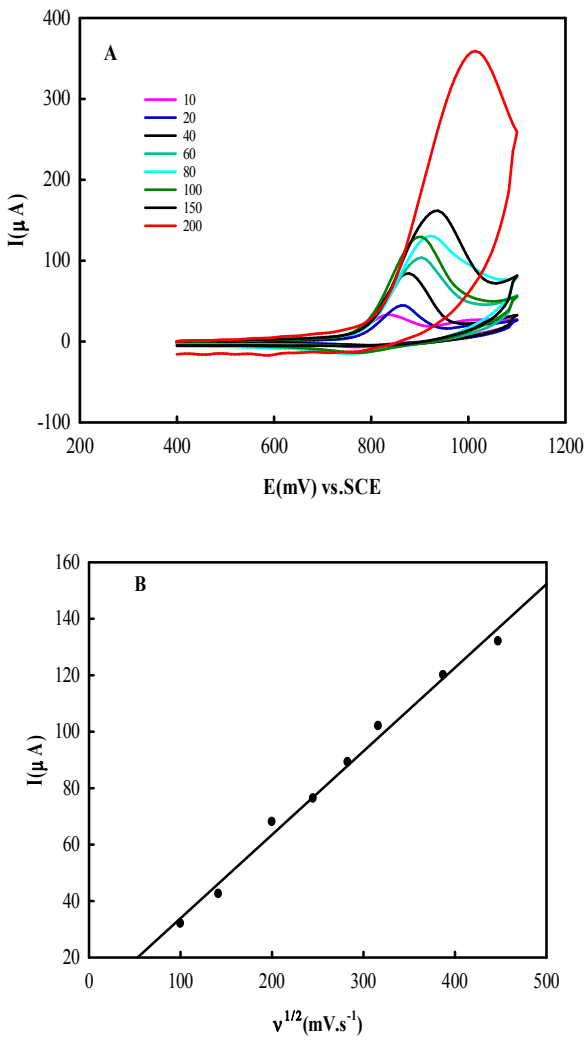

Fig. 8. (A) CVs of 0.01 mM famotidine at 3-MPA/Au-DNSs/GCE in pH 2.0, at different potential scan rates (10 to 200 mV s^{-1}). (B) Variation of E_p *vs.* logυ.

5 min. Before reaching to adsorption equilibrium, the peak current was improved by increasing time. However, after 5 min, the intensity of signal tended to decrease, demonstrating that adsorption equilibrium was gained at 5 min and all binding sites were filled by 3-MPA. So, the adsorption time of 5 min was used for further study (see Fig. 7B).

Effect of Potential Scan Rate

The cyclic voltammetric technique was used to study electrooxidation of 1.0 mM famotidine at 3-MPA/Au-DNSs/GCE in buffer solution with pH 2.0 (0.1 M phosphate), at various potential scan rates (10 to 200 mV s^{-1}) (in optimized condition) (Fig. 8A). The oxidation peak current and the scan rate (υ) exhibits a linear

relationship, demonstrating that the oxidation of famotidine at the surface of 3-MPA/Au-DNSs/GCE followed an adsorption-controlled mechanism (Fig. 8B).

$$I_{pa}\,(\mu A) = 295.2\,\upsilon^{1/2}\,(V\,s^{-1})^{1/2} + 4.3 \quad (R^2 = 0.999) \qquad (2)$$

The linear relation between peak potential and logarithm of scan rate was demonstrated as the following equation:

$$E_p\,(V) = 1.075 + 0.1206\,\log\upsilon\,(V\,s^{-1}) \quad (R^2 = 0.992) \quad (3)$$

According to Laviron equation in an irreversible electrode process, the number of electrons transferred in the electrooxidation of famotidine can be calculated by the following equation:

$$E_p\,(V) = E^{\circ} + \left(\frac{2.303RT}{(1-\alpha)nF}\right)\log\left(\frac{RTK^{\circ}}{(1-\alpha)nF}\right) + \left(\frac{2.303RT}{(1-\alpha)nF}\right)\log v\,(VS^{-1}) \qquad (4)$$

υ: scan rate, α: the transfer coefficient, n: number of electrons transferred, k^o: standard heterogeneous rate constant of the reaction, and E^o: formal redox potential. The value of αn is evaluated from the slope of E_p *vs.* logv and the slope was 0.1206 and αn was 0.49 (T = 298 K, R = 8.314 J K^{-1} mol^{-1} and F = 96480 C). In an irreversible system, α was assumed to be 0.5. So, in rate determining step, n was evaluated to be ~1.0.

Analytical Measurements

CV method was used to quantitative analysis of famotidine. In contrast to response signals obtained by differential pulse voltammetry (DPV), cyclic voltammograms present better shape in determination of famotidine [18]. CV measurements were performed in buffer solution with pH 2.0 (0.1 M phosphate) as supporting electrolyte, in concentration range of 3.0×10^{-7}-1.0×10^{-5} M at 3-MPA/Au-DNSs/GCE (Fig. 9A). The oxidation peak current was improved by increasing the concentration of famotidine in the range of 3.0×10^{-7}-1.0×10^{-5} M linearly. The calibration curve is demonstrated in Fig. 9B. The detection limit for determination famotidine was 3.33×10^{-8} M (for S/N = 3) based on the optimum conditions, respecting Eq. (5).

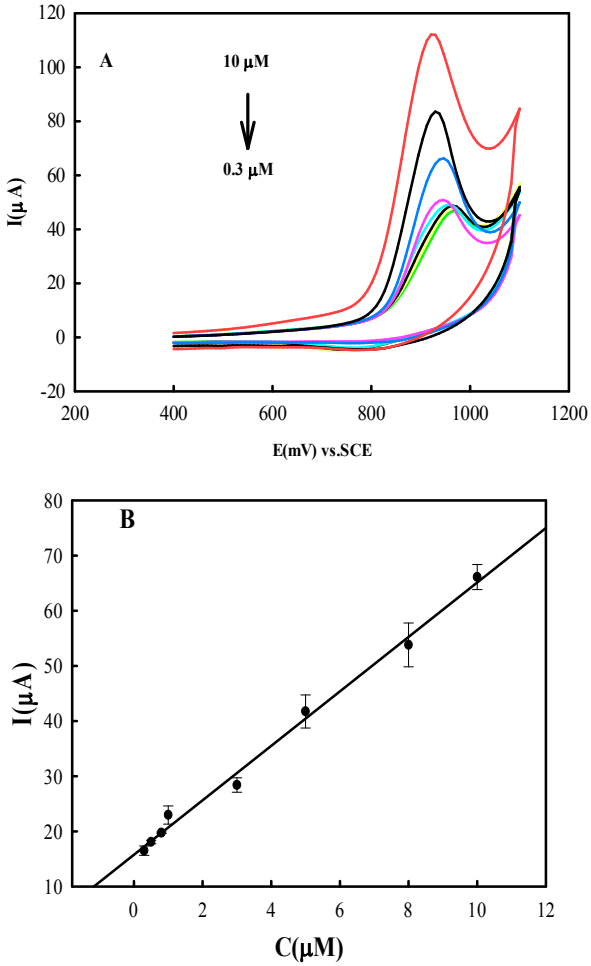

Fig. 9. (A) Cyclic voltammograms of various concentrations of famotidine at 3-MPA/Au-DNSs/GCE in pH 2.0, at potential scan rate 100 mV s^{-1}.

$$I_p/\mu A = 15.292 + (5.194\,C) \quad (R^2 = 0.996,\ C \text{ is in } (5.194\,C)\ \mu M) \qquad (5)$$

Table 2 compares the sensing performance of 3-MPA/Au-DNSs/GCE with other famotidine sensors. The presented mercury-free method demonstrated wider linear range and good detection limit.

The reproducibility of the modified electrode was studied in two concentration levels of famotidine (1.0×10^{-5} M and 5.0×10^{-6} M) in buffer solution pH 2.0 and the sweep rate was 100 mV s^{-1} by using CV for ten repeated

Table 2. Analytical Results of Electrochemical Sensors in Determination of Famotidine

Electrode	DLR (M)	LOD (M)	Method	Ref.
Ultra trace graphite electrode	2.0×10^{-6}-9.0×10^{-5}	3.73×10^{-7}	DPV	[18]
Disposable pencil graphite electrode	4.72×10^{-7}-4.95×10^{-4}	1.5×10^{-7}	DPV	[15]
Nanocrystalline graphite-like Pyrolytic carbon Film electrode	2.0×10^{-7}-32×10^{-6}	7.0×10^{-8}	CV	[17]
flower-like nickel hydroxide nanosheets/CPE	20×10^{-6}-140×10^{-6}	5.91×10^{-6}	Amperometry	[13]
3-MPA/Au-DNSs/GCE	1.0×10^{-7}-1.0×10^{-5}	3.33×10^{-8}	CV	This work

CPE: carbon paste electrode.

measurements. The relative standard deviations for famotidine determination, based on the ten replicates of analysis were 0.65%, 0.86% for 1.0×10^{-5} M and 5.0×10^{-6} M, respectively.

The applicability of 3-MPA/Au-DNSs/GCE in determination of famotidine in real samples such as human serum was studied by using the standard addition method. Respecting Eq. (6), the slope of the calibration curve was obtained by spiking standard solution of famotidine in concentration range of 3.0×10^{-7}-1.0×10^{-5} M, the slope calculated to be 5.44 μA μM^{-1} with a correlation coefficient of (R^2) 0.9973. Compared with the slope of the standard curve (5.194 μA μM^{-1}), a recovery of 104.8% was evaluated, demonstrating high applicability of 3-MPA/Au-DNSs/GCE in accurate determination of famotidine in complex human serum samples.

Also, the standard addition method was used to study the applicability of 3-MPA/Au-DNSs/GCE in determination of famotidine in a commercial tablet. A defined amount of famotidine pharmaceutical sample was spiked in different concentrations ranging from 3.0×10^{-7} to 1.0×10^{-5} M. The slope of the calibration curve was calculated to be 5.242 μA μM^{-1} with a correlation coefficient of (R^2) 0.9916. By comparing two slopes of the standard and spiked pharmaceutical sample, a recovery of 100.90% was calculated, revealing high sensitivity of proposed electrode in detection of famotidine in the presence of the tablet matrix.

CONCLUSIONS

New and high performance 3-MPA/Au-DNSs nanocomposite was designed in this study. High efficiency of 3-MPA/Au-DNSs/GCE in famotidine sensing was attributed to enhanced active surface area, amplified charge transfer rate and high electrocatalytic activity of 3-MPA/Au-DNSs. CV method was used to determine famotidine with high sensitivity in a wide linear range of 3.0×10^{-7}-1.0×10^{-5} M with a good detection limit of 3.33×10^{-8} M. 3-MPA/Au-DNSs/GCE was prepared fast and simple *via* an inexpensive and environmentally friendly method. 3-MPA/Au-DNSs/GCE was successfully applied in detection of famotidine in the presence of the tablet matrix and complex human serum samples that demonstrated high capability for further application in pharmaceutical and clinical industry. In addition, 3-MPA/Au-DNSs-based sensors possess high potential for sensitive and rapid on-site monitoring of famotidine, and can be considered as an interesting alternative for conventional analysis methods such as chromatography and spectroscopy.

ACKNOWLEDGMENTS

The authors gratefully acknowledge the support of this work by University of Mohaghegh Ardabili research council, Ardabil, Iran.

REFERENCES

[1] S. Skrzypek, W. Ciesielski, A. Sokołowski, S. Yilmaz, D. Kaźmierczak, Talanta 66 (2005) 1146.

[2] V. Garzón, D.G. Pinacho, R.-H. Bustos, G. Garzón, S. Bustamante, Biosensors 9 (2019) 132.

[3] M. Hanif, N. Nazer, V. Chaurasiya, U. Zia, TJPR 15 (2016) 605.

[4] X. Wang, E. Rytting, D.R. Abdelrahman, T.N. Nanovskaya, G.D. Hankins, M.S. Ahmed, Biomed. Chromatogr. 27 (2013) 866.

[5] S.A. Majidano, M.Y. Khuhawar, Chromatographia 75 (2012) 1311.

[6] N. Helali, N. Tran, L. Monser, M. Taverna, Talanta 74 (2008) 694.

[7] K. Basavaiah, O. Zenita, Química Nova 34 (2011) 735.

[8] N.R. Reddy, K. Prabhavathi, Y.B. Reddy, I. Chakravarthy, Indian J. Pharm. Sci. 68 (2006) 645.

[9] A.I. Hassan, Acta Chemica Iasi 27 (2019) 47.

[10] A.A. Al-Shibly, H.H. Monir, M.R. El-Ghobashy, S.M. Amer, Eur. J. Org. Chem. 7 (2016) 161.

[11] A. El-Bayoumi, A. El-Shanawany, M. El-Sadek, A.A. El-Sattar, Spectrosc. Lett. 30 (1997) 25.

[12] L. Zhong, R. Eisenhandler, K.C. Yeh, Int. J. Mass Spectrom. 36 (2001) 736.

[13] R. Dehdari Vais, H. Yadegari, H. Heli, Iran. J. Pharm. Res. 19 (2020) 120.

[14] S. Maleki, T. Madrakian, A. Afkhami, Talanta 181 (2018) 286.

[15] I.G. David, D.E. Popa, A.-A. Calin, M. Buleandra, E.-E. Iorgulescu, Turk. J. Chem. 40 (2016) 125.

[16] N.R. Stradiotto, H. Yamanaka, M.V.B. Zanoni, J. Braz. Chem. Soc. 14 (2003) 159.

[17] M. Hadi, A. Ehsani, E. Honarmand, Electroanalysis 29 (2017) 756.

[18] S. Yagmur, S. Yilmaz, G. Saglikoglu, B. Uslu, M. Sadikoglu, S.A. Ozkan, J. Serb. Chem. Soc. 79 (2014) 53.

[19] M.I. Walash, M.K. Sharaf-El-Din, M.E.S. Metwally, M.R. Shabana, J. Chin. Chem. Soc. 52 (2005) 927.

[20] M. Amiri, F. Rezapour, A. Bezaatpour, J. Electroanal. Chem. 735 (2014) 10.

[21] K. Nekoueian, M. Amiri, M. Sillanpää, F. Marken, R. Boukherroub, S. Szunerits, Chem. Soc. Rev. 48 (2019) 4281.

[22] W.T. dos Santos, R.G. Compton, Sens. Actuators B Chem. 285 (2019) 137.

[23] M. Amiri, E. Amali, A. Nematollahzadeh, Sens. Actuators B Chem. 216 (2015) 551.

[24] G. Muthusankar, C. Rajkumar, S.-M. Chen, R. Karkuzhali, G. Gopu, A. Sangili, N. Sengottuvelan, R. Sankar, Sens. Actuators B Chem. 281 (2019) 602.

[25] M. Amiri, S. Sohrabnezhad, A. Rahimi, Mater. Sci. Eng. C 37 (2014) 342.

[26] M.B. Gholivand, E. Ahmadi, M. Mavaei, Sens. Actuators B Chem. 299 (2019) 126975.

[27] M. Amiri, S. Nouhi, Y. Azizian-Kalandaragh, Mater. Chem. Phys. 155 (2015) 129.

[28] M. Amiri, M. Alimoradi, K. Nekoueian, A. Bezaatpour, Ind. Eng. Chem. Res. 51 (2012) 14384.

[29] D. Tonelli, E. Scavetta, I. Gualandi, Sensors 19 (2019) 1186.

[30] S.R. Torati, K.C. Kasturi, B. Lim, C. Kim, Sens. Actuators B Chem. 243 (2017) 64.

[31] N. Manjubaashini, P.J. Sephra, K. Nehru, M. Sivakumar, T.D. Thangadurai, Sens. Actuators B Chem. 281 (2019) 1054.

[32] J. Wang, J. Yang, P. Xu, H. Liu, L. Zhang, S. Zhang, L. Tian, Sens. Actuators B Chem. 306 (2020) 127590.

[33] Y. Pei, M. Hu, Y. Xia, W. Huang, Z. Li, S. Chen, Sens. Actuators B Chem. 304 (2020) 127416.

[34] H. Han, D. Pan, C. Wang, R. Zhu, RSC Adv. 7 (2017) 15833.

[35] J. Fang, X. Ma, H. Cai, X. Song, B. Ding, Nanotechnology 17 (2006) 5841.

[36] E. Rafatmah, B. Hemmateenejad, Sens. Actuators B Chem. 304 (2020) 127335.

[37] L. Wang, X. Chen, X. Wang, X. Han, S. Liu, C. Zhao, Biosens. Bioelectron. 30 (2011) 151.

[38] M.H. Mashhadizadeh, A. Azhdeh, N. Naseri, J. Electroanal. Chem. 787 (2017) 132.

[39] J. Kochana, K. Starzec, M. Wieczorek, P. Knihnicki, M. Góra, A. Rokicińska, P. Kościelniak, P. Kuśtrowski, J. Solid State Electrochem. 23 (2019) 1463.

[40] M. Bełtowska-Brzezinska, A. Zmaczyńska, T. Łuczak, Electrocatalysis 7 (2016) 79.

[41] H. Salehniya, M. Amiri, Y. Mansoori, RSC Adv. 6 (2016) 30867.
[42] S. Yu, H. Li, G. Li, L. Niu, W. Liu, X. Di, Talanta 184 (2018) 244.
[43] M. Shanmugam, K. Kim, J. Electroanal. Chem. 776 (2016) 82.